



Generation of polarization-entangled photon pairs in a cold atomic ensemble

Yuelong Wu · Shujing Li · Wei Ge ·
Zhongxiao Xu · Long Tian · Hai Wang

Received: 21 October 2015 / Revised: 8 December 2015 / Accepted: 18 December 2015 / Published online: 20 January 2016
© Science China Press and Springer-Verlag Berlin Heidelberg 2016

Abstract We report an experimental generation of polarization-entangled photon pairs in a cold atomic ensemble. A single Stokes photon and one spin-wave excitation are simultaneously created via spontaneous Raman scattering. The spin-wave excitation is then converted into an anti-Stokes photon via an electromagnetic-induced-transparency reading process. The measured cross-correlation functions between the Stokes and anti-Stokes photons for two orthogonal polarizations are ~ 75 and 74 , respectively, at a generation rate of the photon pair of $\sim 60/s$. Based on such correlations, we obtain polarization-entangled photon pairs, whose Bell parameter is $S = 2.77 \pm 0.01$, violating Bell-CHSH inequality by ~ 77 standard deviations. The presented polarization-entangled photon source has high entanglement degree and fast generation rate, which will promise us to apply it in future quantum repeater.

Keywords Polarization-entangled photon pairs · Spontaneous Raman scattering · Cold atomic ensemble · Cross-correlation function · Bell parameter · Spin-wave excitation

1 Introduction

The polarization-entangled photon pairs capable of storages play a critical role in quantum information processing, quantum computation and quantum communication [1–8]. The spontaneous parameter down-conversion (SPDC) in nonlinear crystals has been widely used to generate polarization-entangled photon pairs [9–12]. However, the obtained entangled states from SPDC are unfeasible to be directly stored in most matter nodes due to their large linewidth of THz order [2, 11]. Spontaneous Raman scattering (SRS) in an atomic ensemble can emit a single Stokes photon and simultaneously create one spin-wave excitation [2]. The cross-correlation between the Stokes photons and the spin-wave excitations allows people to achieve the spin-wave-photon entanglement [4]. The single spin-wave excitation can be mapped into a single anti-Stokes photon via dynamic electromagnetic-induced-transparency (EIT) reading process. The generated Stokes and anti-Stokes photons are narrow-bandwidth entangled photon pairs which can be effectively stored in atomic ensemble via electromagnetically induced transparency (EIT) [13, 14].

Over the past decades, important progress has been made in generation of polarization-entangled photon pairs by SRS [15–20]. In 2005, Matsukevich et al. [16] reported the experimental generation of entanglement of a photon and a collective atomic excitation in a cloud of cold Rb atoms. Pan's group [17] has demonstrated a stable atom-photon entanglement source for quantum repeaters in 2007. In 2011, Yan et al. [18] reported the generation of non-degenerate narrow-bandwidth paired photons with time-frequency and polarization entanglements from a cloud of cold atoms. In 2014, Liao et al. [19] generated subnatural-linewidth polarization-entangled photon pairs. In 2015,

Y. Wu · S. Li · W. Ge · Z. Xu · L. Tian · H. Wang (✉)
The State Key Laboratory of Quantum Optics and Quantum Optics Devices, Institute of Opto-Electronics, Shanxi University, Taiyuan 030006, China
e-mail: wanghai@sxu.edu.cn

Y. Wu · S. Li · W. Ge · Z. Xu · L. Tian · H. Wang
Collaborative Innovation Center of Extreme Optics, Shanxi University, Taiyuan 030006, China

Ding et al. [20] generated entanglement of a heralded single photon in both path and polarization storage and achieved polarization entanglement storage in two cold Rb atomic ensembles. However, the measured Bell parameters [21] for the polarization-entangled photon pairs in these works are less than ~ 2.6 [17]. The high-quality polarization-entangled photon source still remains challenge.

In this paper, we report an experimental study on generation of polarization-entangled photon pairs via SRS in a cold atomic ensemble. A magnetic field along z -direction is applied to define quantum axis. An appropriate atomic level configuration is chosen to couple the light fields involved in SRS. We use a writing laser pulse to excite the cold atoms; thus, a single Stokes photon and one spin wave are created at the same time. We collected the Stokes photons along z -axis. The spin-wave excitation is then converted into an anti-Stokes photon via an EIT reading process [13] and is collected at the direction opposite to that of the Stokes photons. For verifying photon–photon entanglement, we perform the correlation measurements between the Stokes and anti-Stokes photons at two orthogonal polarization bases (right/left circular polarizations). At a small excitation probability $\chi = 0.014$, the measured cross-correlation functions for two different polarization bases, Bell parameter and generation rate of the pair of Stokes and anti-Stokes photons are $g^{(2)} > 70$, $S = 2.77 \pm 0.01$ and $\sim 60/s$, respectively.

2 Experimental setup

The relevant atomic levels and experimental setup are shown in Fig. 1a, b. A cloud of cold ^{87}Rb atoms is used to generate polarization-entangled photon pairs. The atoms are optically pumped into the initial level $|a\rangle$ by σ^\pm -polarized laser beams P_1 and P_2 (not shown in Fig. 1a), which are overlapped at a PBS and then collinearly go through the atoms at an angle of 2° to the z -axis. The frequencies of P_1 and P_2 are tuned on $|b\rangle \leftrightarrow |e_2\rangle$ and $|b\rangle \leftrightarrow |e_1\rangle$ transitions, respectively. The atoms are prepared in $|a\rangle$ with equal probability in the three Zeeman sublevels $|m_a = -1\rangle$, $|m_a = 0\rangle$ and $|m_a = 1\rangle$. For simplicity, the atoms are assumed to be in $|a, m = 0\rangle$ state. A weak magnetic field \mathbf{B} is applied on the atoms along z -axis. The write light beam goes through the atoms along x -axis, whose frequency is tuned to $|a\rangle \rightarrow |e_2\rangle$ transition with 10 MHz red-detuned. We use acoustic-optical modulator (AOM) to switch on/off the write light beam and then generate a write pulse. Under the action of the write pulse on the atoms, a single Stokes photon will be emitted with a small probability into a spatial field mode S and the spin-wave (SW) A with one excitation will be created simultaneously. The wave vector of the SW mode A is $\vec{k}_A = \vec{k}_w - \vec{k}_S$, where \vec{k}_w and \vec{k}_S

are the wave vectors of write field and Stokes field S , respectively. After a storage time τ , a reading laser pulse with its frequency tuned to $|b\rangle \rightarrow |e_1\rangle$ transition and its propagating direction along x -axis (opposite to that of the write beam) is applied to transfer the SW excitation into a single anti-Stokes photon. The anti-Stokes photon will be in the spatial field mode S' whose wave vector is $\vec{k}_{S'} = -\vec{k}_S$, which means it propagates along the direction opposite to that of Stokes photons.

According to the discussion in Ref. [22], when the Stokes photons are $\sigma^+(\sigma^-)$ polarization, the anti-Stokes photons will be $\sigma^-(\sigma^+)$ polarization, where σ^+/σ^- represents right/left circular polarization. Since the $\sigma^+ - (\sigma^-)$ -polarized Stokes photons are strongly correlated with the $\sigma^- - (\sigma^+)$ -polarized anti-Stokes photons, the Stokes photon and anti-Stokes photon will be well entangled in their polarization states under the condition of excitation probability $\chi \ll 1$.

By inserting a $\lambda/4$ plate in the each path of S and S' modes, respectively, their circular polarizations are transferred into linear polarizations (for Stokes photons $S: \sigma^+(\sigma^-) \rightarrow H(V)$; for anti-Stokes photons $S': \sigma^+(\sigma^-) \rightarrow V(H)$), where H/V represents horizontal/vertical polarization. The ideal entanglement state between the Stokes and anti-Stokes photons can be written as

$$|\psi(\tau)\rangle_{S-S'} = \frac{1}{\sqrt{2}} (|H\rangle_S |H\rangle_{S'} + |V\rangle_S |V\rangle_{S'}), \tag{1}$$

where the relative phase is not considered due to the short storage time [22].

As shown in Fig. 1a, the Stokes and anti-Stokes photons are collected by two single-mode fibers, whose modes S and S' have a $1/e$ diameter of 0.7 mm at the center of the cold atomic cloud. After single-mode fibers, two sets of optical filters, each one including three Fabry–Perot etalons, are used to reduce the background noise to a level of 10^{-4} per write/read pulses. The polarization projection measurement on Stokes (anti-Stokes) photons is completed by using a half-wave plate, a cubic polarization beam splitter and two single-photon detectors D_{H1}, D_{V1} (D_{H2} and D_{V2}). The data from the detectors are recorded and analyzed by a self-programmed coincidence apparatus based on field-programmable gate array (FPGA: NI PXIe-7966R). The z -polarized writing and reading laser beams counter-propagate through the atoms along x -axis, whose diameters (powers) are ~ 3 mm (1 mW) and 3.3 mm (~ 50 mW), respectively, at the center of the atoms.

The time sequence of the experimental procedure is shown in Fig. 1c. The experimental cycle repeats with a frequency of 30 Hz. Each experimental cycle contains a 23-ms preparation stage and a 10-ms experiment run. During the preparation stage, the atomic ensemble is trapped in the MOT for 22 ms and further cooled to a

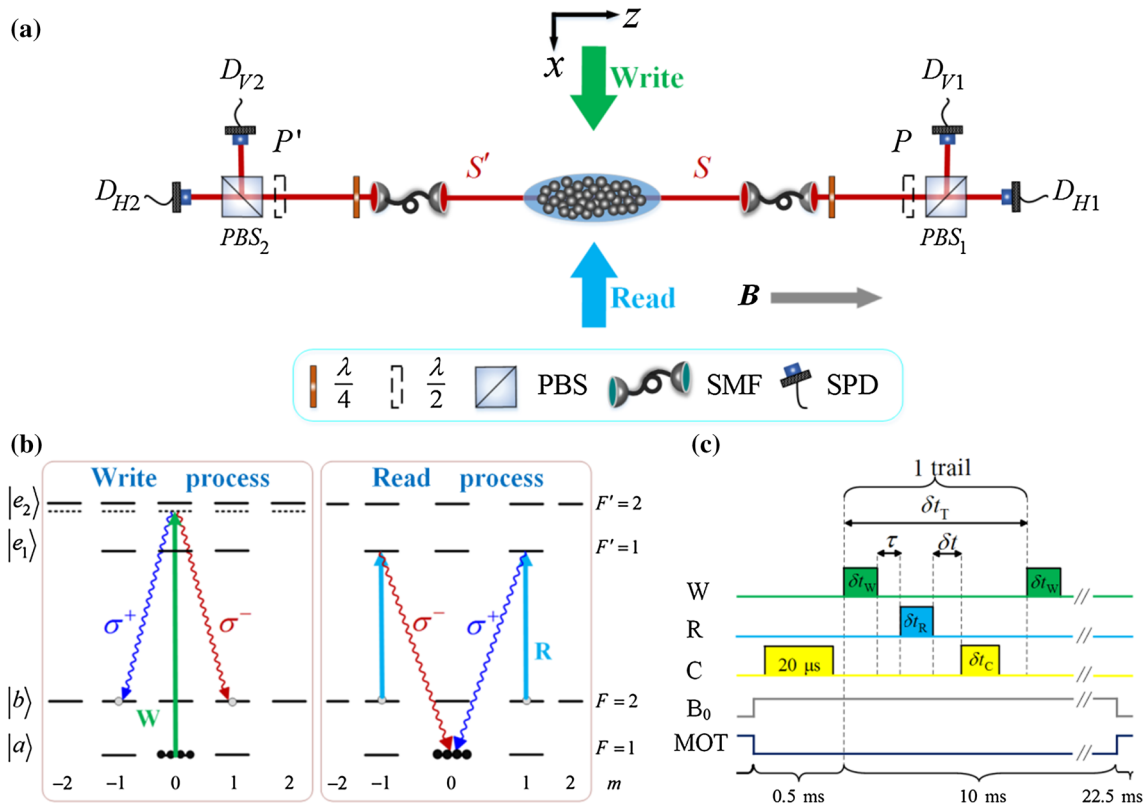


Fig. 1 (Color online) Overview of the experiment. **a** Experimental setup for generating polarization-entangled photon pairs. The magnetic field $B = 200$ mG is applied on the cold atoms along z -axis. The z -polarized write beam goes through the atoms along x -direction, while the z -polarized read beam counter-propagates with respect to the write beam. PBS: polarization beam splitter, SMF: single-mode fiber, SPD: single-photon detector. **b** The scheme of relevant ^{87}Rb atomic levels coupled by light fields of writing (W), reading (R), σ^\pm -polarized Stokes and anti-Stokes photons. **c** The time sequence of an experimental cycle

temperature of ~ 130 μK by a Sisyphus cooling for 0.5 ms. The cloud of atoms has a size of $(\sim 5 \times 2 \times 2)$ mm^3 and an optical density of ~ 7 , whose longitudinal symmetry axis is along z -axis. Then, the MOT (beams and magnetic field) is turned off, and the guiding magnetic field $B = 200$ mG is applied. At the end of this stage, P_1 and P_2 laser beams are switched on for 20 μs to pump the atoms into the level $|a\rangle$. After the preparation stage, the 10-ms experiment run which contains n trails starts. In each trail, a write laser pulse with a length of $\delta t_W = 70$ ns is applied to generate correlated pairs of a single Stokes photon and a single SW excitation. After a storage time τ , a read laser pulse with a length of $\delta t_R = 100$ ns is applied to retrieve the stored SWs. For the case of $\tau = 30$ ns, the 10-ms experimental run contains $n = 10,000$ trails; thus, 1-s experimental sequence contains $N = 300,000$ trails.

3 Results and discussion

We firstly measured the coincidence counts C_{HH} (C_{HV}) between detectors D_{H_1} and D_{H_2} (D_{H_1} and D_{V_2}) as the

function of storage time τ at excitation probability $\chi \approx 0.014$, and the results are shown in Fig. 2. Each data point corresponds to the counts collected in 33 s. At storage time $\tau = 30$ ns, the generation rate of the photon pairs is measured to be $\sim 60/\text{s}$ (C_{VV} is almost the same as C_{HH}). The overall detection efficiency η is $\sim 30\%$, including the coupling efficiency of single-mode fibers (80%), the

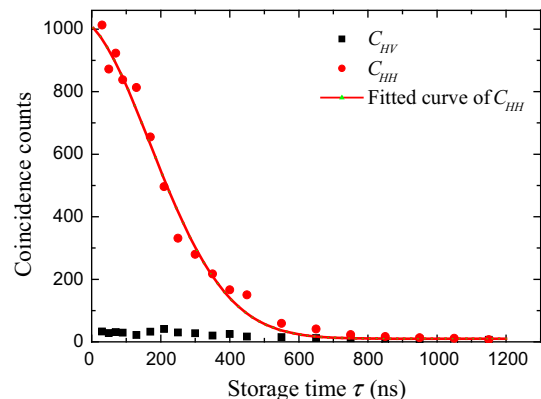


Fig. 2 (Color online) Coincidence counts as a function of storage time τ

filtering efficiency (80 %) and the quantum efficiency of the single-photon detectors (50 %). Considering that the measured retrieval efficiency of the spin wave $R = 20\%$ and the detection efficiency of a single photon η , the theoretical detection rate calculates to be $r = \eta^2 \chi RN = 75/s$ for repetition rate $N = 300,000/s$, which is basically consistent with the experimental value 60/s. The generation rate will be increased further if the retrieval efficiency and the detection efficiency are improved.

The polarization cross-correlation functions of Stokes and anti-Stokes photons are defined as

$$g_{HH(VV)}^{(2)} = \frac{P_{H_1 H_2 (V_1 V_2)}}{P_{H(V_1)} P_{H(V_2)}}, \quad (2)$$

where P_{H_1} (P_{V_1}) and P_{H_2} (P_{V_2}) are the probabilities for detecting a single photon on detector D_{H_1} (D_{V_1}) and D_{H_2} (D_{V_2}), respectively, and $P_{H_1 H_2}$ is the coincidence probability between D_{H_1} and D_{H_2} . D_{H_1} (D_{H_2}) and D_{V_1} (D_{V_2}) is used for detecting H -polarized and V -polarized Stokes (anti-Stokes) photons. Under the excitation probability $\chi \approx 0.014$, the measured $g_{HH}^{(2)}$ and $g_{VV}^{(2)}$ are 75 and 74, which are far beyond the limit of 2.

In order to evaluate the entanglement state $|\Psi\rangle_{S'-S}$, we measure the correlations between the anti-Stokes and Stokes photons $E(\theta_p, \theta_{p'})$ [16] as the function of θ_p and $\theta_{p'}$, where θ_p and $\theta_{p'}$ are the polarization angles of the Stokes photon in S mode and anti-Stokes photon in S' mode, respectively. Their values can be changed by two half-wave plates P and P' (Fig. 1a), respectively. At storage time $\tau = 30$ ns, the measured $E(\theta_p, \theta_{p'})$ as the function of $\theta_{p'}$ for fixed θ_p is shown in Fig. 3. The interference visibility of the polarization correlation is 97.1 %.

In the canonical settings $\theta_p = 0^\circ$, $\theta_{p'} = 22.5^\circ$, $\theta'_p = 45^\circ$ and $\theta'_{p'} = 67.5^\circ$, the Bell parameter S for the entanglement state $|\Psi(\tau)\rangle_{S'-S}$ is $S = 2.77 \pm 0.01$ (2.12 ± 0.03) for the storage time of $\tau = 30$ ns (930 ns), which significantly

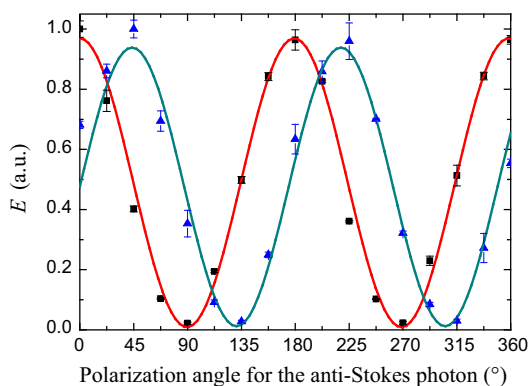


Fig. 3 (Color online) Normalized polarization correlation of the paired Stokes and anti-Stokes photons. The squares (triangles) correspond to the data of $\theta_p = 0^\circ$ ($\theta'_p = 45^\circ$). The solid lines are sinusoidal fitting lines

violates the Bell-CHSH inequality by ~ 77 standard deviations. The measured Bell parameter as the function of storage time τ is shown in Fig. 4, which shows that the polarization-entangled photon pair can be generated after a controllable storage time.

We performed quantum state tomography to fully characterize the two-photon entangled state. The polarization analyzer is composed of HWP, QWP and PBS. After the PBS, the photons are coupled into single-mode fibers and detected by SPDs. We used the measurement bases $|H\rangle$, $|V\rangle$, $|R\rangle$, $|L\rangle$, $|D\rangle$ and $|A\rangle$ for each photon, where the six bases denote horizontal, vertical, right circular, left circular, diagonal (45°) and antidiagonal (-45°) polarizations, respectively. Thus, a total of 36 two-photon polarization bases should be measured. Since each photon employs two SPDs, the measurement basis and its perpendicular basis can be recorded at the same time. The 36 measurement bases can be measured from 9 polarization settings. Each of the polarization setting is measured over 33–66 s for different storage times. Using the measured data of the 36 bases, we reconstructed the density matrix ρ of the two-photon entangled state by maximum likelihood technique [23] for different storage times. The fidelity with the ideal state $|\Psi(\tau)\rangle_{S'-S} = \frac{1}{\sqrt{2}}(|H\rangle_{S'}|H\rangle_S + |V\rangle_{S'}|V\rangle_S)$ is also calculated through the equation $F = \text{Tr}(\sqrt{\sqrt{\rho}\rho_{\text{ideal}}\sqrt{\rho}})^2$, where ρ_{ideal} is the density matrix of the ideal state. The measured fidelities versus storage time are shown in Fig. 5. The results show that the fidelity is $96.5\% \pm 0.3\%$ at $\tau = 30$ ns. The errors on the fidelities are estimated using a 100-run Monte Carlo simulation.

4 Conclusions

We generate polarization-entangled photon pairs via SRS in a cold ^{87}Rb atomic ensemble. With an appropriate atomic level configuration and experimental arrangement,

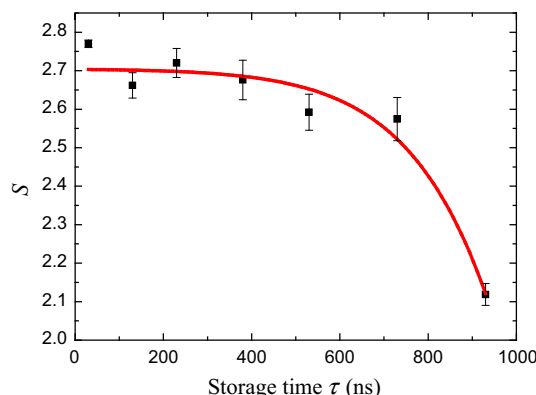


Fig. 4 (Color online) Measured values of the Bell parameter S as a function of storage time τ

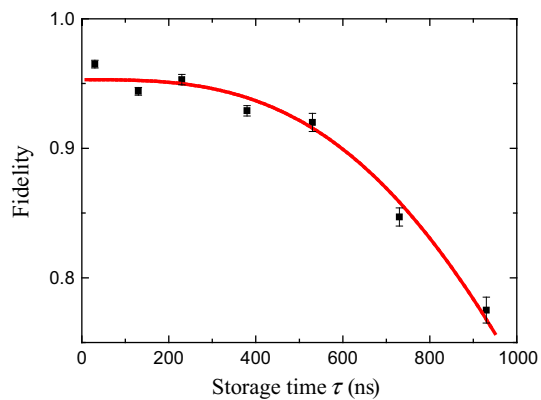


Fig. 5 (Color online) Fidelity of the measured entangled two-photon state as a function of storage time τ

the measured results present good nonclassical correlation $g^{(2)} > 70$ and the measured Bell parameter $S = 2.77 \pm 0.01$. The pair generation rate is up to $\sim 60/s$. Such high entanglement degree and fast generation rate of photon pairs will allow the polarization-entangled photon source to play a crucial role in future quantum information processing based on quantum networks.

Acknowledgments This work was supported by the National Basic Research Program of China (2010CB923103) and the National Natural Science Foundation of China (11475109, 11274211 and 60821004).

Conflict of interest The authors declare that they have no conflict of interest.

References

- Pan JW, Chen ZB, Lu CY et al (2012) Multi-photon entanglement and interferometry. *Rev Mod Phys* 84:777–838
- Sangouard N, Simon C, Riedmatten H et al (2011) Quantum repeaters based on atomic ensembles and linear optics. *Rev Mod Phys* 83:33–80
- Zhao B, Chen ZB, Chen YA et al (2007) Robust creation of entanglement between remote memory qubits. *Phys Rev Lett* 98:240502–240505
- Chen ZB, Zhao B, Chen YA et al (2007) Fault-tolerant quantum repeater with atomic ensembles and linear optics. *Phys Rev A* 76:022329
- Guo WJ, Fan DH, Wei LF (2015) Experimentally testing bell's theorem based on hardy's nonlocal ladder proofs. *Sci China Phys Mech Astron* 58:024201
- Dong YC, Liu BH, Wang Z et al (2015) Multiuser-to-multiuser entanglement distribution based on 1550 nm polarization-entangled photons. *Sci Bull* 60:1128–1132
- Wang F, Luo MX, Chen XB et al (2014) Typical universal entanglers. *Sci China Phys Mech Astron* 57:1913–1917
- Heilmann R, Gräfe M, Nolte S et al (2015) A novel integrated quantum circuit for high-order W-state generation and its highly precise characterization. *Sci Bull* 60:96–100
- Kwiat PG, Mattle K, Weinfurter H et al (1995) New high-intensity source of polarization-entangled photon pairs. *Phys Rev Lett* 75:4337–4341
- Lu CY, Zhou XQ, Gühne O et al (2007) Experimental entanglement of six photons in graph states. *Nat Phys* 3:91–95
- Akiba K, Kashiwagi K, Arikawa M et al (2009) Storage and retrieval of nonclassical photon pairs and conditional single photons generated by the parametric down-conversion process. *New J Phys* 11:013049
- Hamel DR, Shalm LK, Hübel H et al (2014) Direct generation of three-photon polarization entanglement. *Nat Photon* 8:801–804
- Wang H, Xie CD, Peng KC (2012) Quantum storage of optical signals and coherent manipulation of quantum states based on electromagnetically induced transparency. *Chin Sci Bull* 57:1893–1902
- Zhou SY, Zhang SC, Liu C et al (2012) Optimal storage and retrieval of single-photon waveforms. *Opt Express* 20:24142–24149
- Minár J, Riedmatten HD, Sangouard N (2012) Quantum repeaters based on heralded qubit amplifiers. *Phys Rev A* 85:032313
- Matsukevich DN, Chanelière T, Lan SY et al (2005) Entanglement of a photon and a collective atomic excitation. *Phys Rev Lett* 95:040405
- Chen S, Chen YA, Zhao B et al (2007) Demonstration of a stable atom-photon entanglement source for quantum repeaters. *Phys Rev Lett* 99:180505
- Yan H, Zhang S, Chen JF et al (2011) Generation of narrow-band hyperentangled nondegenerate paired photons. *Phys Rev Lett* 106:033601
- Liao KY, Yan H, He JY et al (2014) Subnatural-linewidth polarization-entangled photon pairs with controllable temporal length. *Phys Rev Lett* 112:243602
- Ding DS, Zhang W, Zhou ZY et al (2015) Raman quantum memory of photonic polarized entanglement. *Nat Photon* 9:332–338
- Li M, Fei SM, Li-Jost XQ (2011) Bell inequality, separability and entanglement distillation. *Chin Sci Bull* 56:945–954
- Wu YL, Tian L, Xu ZX et al (2015) Simultaneous generation of two spin-wave-photon entangled states in an atomic ensemble. [arXiv:1509.03159](https://arxiv.org/abs/1509.03159)
- JamesDFV Kwiat PG, Munro WJ et al (2001) Measurement of qubits. *Phys Rev A* 64:052312